Vortex Modeling of Single and Multiple Dilution Jet Mixing in a Cross Flow

A. R. Karagozian,* T. T. Nguyen,† and C. N. Kim†
University of California, Los Angeles, Los Angeles, California

An analytical model for the behavior of normally injected jets in a cross flow is developed and applied to fluids of differing densities. Central to the model are the dynamics of the vortex pair structure associated with the local jet cross section and the entrainment of cross flow by jet fluid. Two specific cases are modeled: one involving a single (hot or cold) jet in a cross flow, in which trajectories are found to scale primarily with jet-to-cross flow momentum ratio, and the other involving a series of spanwise jets injected into a cross flow, which indicates scaling with momentum ratio and with the spacing-to-orifice-diameter ratio. In the case of multiple jet penetration, however, merging of the jets into an approximately two-dimensional jet downstream of injection is observed for low spacing-to-diameter ratios.

Nomenclature

$a(t)$ = radius of viscous core
d = orifice diameter
e = local entrainment parameter
F_y = "lift" force acting to separate vortices
$h(t)$ = half-spacing of vortices
k = virtual mass coefficient for motion of vortex cores
ℓ = spanwise spacing of multiple injected jets
L = characteristic length for transverse jet, $= Rd$
P = impulse per unit depth of transverse jet
R = square root of jet-to-cross flow momentum ratio, $\sqrt{\rho_{j0}U_j^2/\rho_\infty U_\infty^2}$
Re = characteristic Reynolds number, $(U_\infty L/\nu)$
t = flow time parameterizing location of vortex pair along trajectory
$T_c(t)$ = temperature of fluid in viscous core
T_{j0} = temperature of jet at orifice
T_∞ = temperature of cross flow
$U(t)$ = cross flow velocity in reference frame of vortices
$U_I(t)$ = induced velocity of infinite row of vortex pairs
U_∞ = cross flow velocity (absolute frame)
U_j = jet velocity at the orifice
$u_v(t)$ = mass-averaged velocity of fluid in jet along trajectory
$v_r(r,t)$ = radial velocity field exterior to viscous core
$w(z,t)$ = complex potential in vortex pair reference frame
X = downstream location of vortex pair
Z = transverse location of vortex pair
$\Gamma_0(t)$ = total (integrated) circulation of each vortex
ν = average eddy viscosity
$\rho_c(t)$ = density of fluid in vortex cores
$\rho_j(t)$ = density of fluid in recirculation cell (except in cores)
ρ_{j0} = density of jet at the orifice
ρ_∞ = density of cross flow
ϕ_v = angle describing orientation of vortex pair

Introduction

ENTRAINMENT and turbulent mixing by jets injected into a cross flow have been studied rather extensively in recent years, primarily through experiments[1-3] and semi-empirical[4,5] or numerical modeling.[6] One motivation for these studies has been the existence of this type of flowfield in the dilution zone of gas turbine combustors, whereby cold diluent air is injected normally into a primary stream of hot combustion products in order to form a suitable temperature profile at the turbine inlet. It has been of continuing interest to determine the effects of varying flow properties, such as jet or cross-flow velocities and temperatures, and geometric parameters, such as lateral spacing of jets, on velocity and temperature distributions at the combustor exit.

To this end, a vortex model of the behavior of a single, isothermal transverse jet has been developed and is described in a recent paper.[7] The model places particular emphasis on the contra-rotating vortex pair associated with the jet cross section, shown schematically in Fig. 1. A distinguishing feature of this representation is that it describes generation of a component of vorticity dominating the near field of the jet as well as a component of vorticity dominating the far field of the jet. The near field component of vorticity is aligned parallel to the jet axis and arises from the deflection of cross flow about the circular orifice. The far field component is aligned parallel to the cross flow and is an outcome of the effective impulse of the deflected jet. This representation is not intended to be a detailed solution of the governing equation for this three-dimensional flow, but instead, it is a locally two-dimensional, viscous model of the important features of the flow. As the vortices separate downstream, cross flow is entrained into the cross section of the

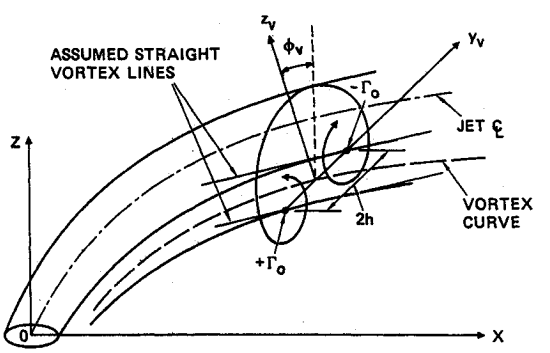

Fig. 1 Description of a locally two-dimensional vortex pair in the field of a single transverse jet.

Received Aug. 19, 1985; revision received Jan. 21, 1986.

*Assistant Professor, Department of Mechanical, Aerospace, and Nuclear Engineering. Member AIAA.
†Graduate Student, Department of Mechanical, Aerospace, and Nuclear Engineering.

jet, approximated as the recirculation cell of the vortices. Cell area then increases downstream, with the results for trajectories giving close correspondence to experiments. In fact, when extended to the situation in which the jet fluid and crossflow react to form a product[8] (again, with the assumption of incompressibility), the vortex model yields results for "flame" lengths that very closely approximate reaction experiments performed in liquid.[9]

The current work examines the considerably more complicated situations in which density variation is taken into account (thus, representing the actual dilution jet problem), and in which a series of dilution jets, aligned in the spanwise direction, is injected into the cross flow, yielding multiple jet interactions.

Dilution Jet Model and Results

When the transversely injected jet and the cross flow are of different densities, the dynamics of the vortex pair associated with the jet is complicated in many respects. Not only does the density of the jet vary along its path; but also, due to the nature of entrainment of the cross flow, the density distribution within the jet cross section itself is nonuniform. Experimental evidence from temperature contours within the cross section[1] indicates that the jet fluid tends to be concentrated in the centers of the vortex structures, while the mixed fluid lies closer to the edge of the vortex pair recirculation cell. On this basis, the density of the viscous vortex cores is assumed to differ from that of the rest of the recirculation cell and that of the cross flow.

A schematic representation for the dilution jet cross section is shown in Fig. 2, where ρ_c represents the density of the viscous cores, ρ_j the density of the remainder of the recirculation cell, and ρ_∞ the density of the cross flow. Due to entrainment of cross flow by the jet, ρ_c and ρ_j will actually vary with flow time t, which is used to parameterize the trajectory of the vortex pair. Again, the local jet curvature is neglected in this model, and the vortices are assumed to be present. While modeling of flow about this jet cross section may be accomplished by superposition of the pair of vortices of strengths $\pm\Gamma_0$, a time-dependent cross flow $U(t) = U_\infty \sin\phi_v(t)$, and the radially growing viscous cores [of radius $a(t)$], the discontinuity in density within the recirculation cell must also be represented.

Assuming inviscid flow exterior to the cores, the complex velocity potential $w(z,t)$ thus may be written for the vortex pair flowfield:

$$w(z,t) = U(t)z + \frac{i\Gamma_0}{2\pi}\ln\left[\frac{z}{z+i2h(t)}\right] + U(t)a^2(t)\left[\frac{1}{z}+\frac{1}{(z+i2h(t))}\right] \tag{1}$$

In this expression, the first term on the right side of the equation represents the freestream, the second term represents the contra-rotating vortices, and the third term represents the two viscous cores. The Extended Blasius Theorem[10] then can be used to compute the forces acting on the cores. This yields a component of "lift" force F_y acting to separate the vortices,

$$\frac{F_y}{\text{depth}} = \rho_j\left[\frac{-\Gamma_0^2}{4\pi h} - \frac{\pi U^2(t)a^4}{2h^3} + U(t)\Gamma_0 + \frac{U(t)\Gamma_0 a^2}{2h^2} + \pi a^2\frac{d^2h}{dt^2}\right] \tag{2}$$

This force now can be set equal to the change with respect to time of momentum associated with a given core,

$$\frac{d}{dt}\left[(\rho_c(t) + k\rho_j(t))\pi a^2(t)\frac{dh}{dt}\right]$$

where k is the virtual mass coefficient of the radially growing viscous core with circulation in an unsteady flowfield. As has been described,[7] an average value of the virtual mass coefficient for the trajectory of the vortex pair can be taken to be $k=4$ (assumed constant with time). The final governing equation for vortex-pair half-spacing $h(t)$ then evolves into

$$\frac{d^2h}{dt^2} + \left[\left(\frac{d\rho_c}{dt} + k\frac{d\rho_j}{dt}\right) + \frac{2}{a}\frac{da}{dt}(\rho_c + k\rho_j) \div (\rho_c + (k-1)\rho_j)\right]\frac{dh}{dt} + \left[\frac{\rho_j}{\rho_c + (k-1)\rho_j}\right]\left[\frac{\Gamma_0^2}{8\pi^2h^3}\right]\left[1 - \frac{a^2}{4h^2}\right] = 0 \tag{3}$$

solution of which requires information concerning the unknown quantities $a(t)$, $\rho_c(t)$, $\rho_j(t)$, and $\Gamma_0(t)$.

By definition, the growth of the viscous core arises from the diffusion of vorticity; and, in theory, this is not directly affected by the change in density that occurs due to mixing. Hence, the approximation of the Gaussian viscous vortex takes the form of a viscous core (with "solid body" rotation) and a potential vortex exterior to the core. This combination is known as the Rankine combined vortex. On this basis, the core radius $a(t)$ is expressed through the relation

$$a(t) = C\sqrt{4\nu t} \tag{4}$$

where from the single vortex analysis, $C = 1.121$. The viscosity ν is considered in this model to be an average turbulent quantity for the cross flow and jet, roughly 1000 times the laminar kinematic viscosity. Calculations indicate that variation by an order of magnitude in the value chosen for ν (or for a characteristic Reynolds number) does not significantly affect the final jet trajectories.[7]

Variation in the densities ρ_c and ρ_j with time (or with distance along the jet) may be derived by considering the nature of entrainment of cross flow by the jet. The description here applies to the cold dilution jet, but it is analogous

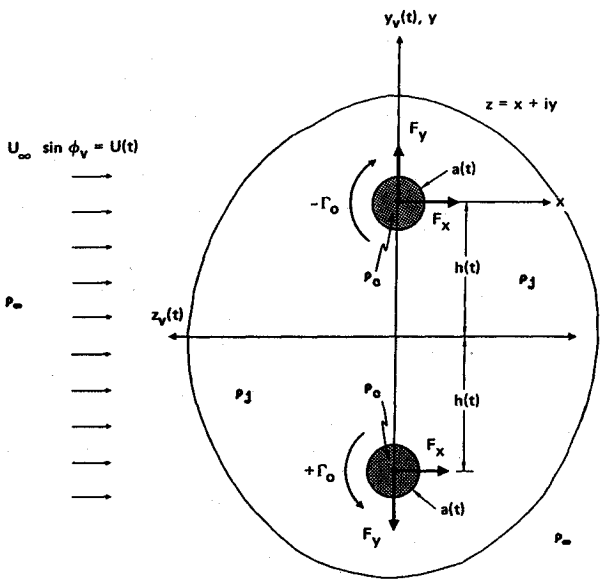

Fig. 2 Local flowfield, density distribution, and forces in vicinity of vortex pair for dilution jet.

to the hot jet in a cold cross flow. In this problem, core growth leads to an increase in the actual mass of the core, with a reduction in its density due to entrainment of and mixing with the warmer fluid within the jet cross section. Similarly, growth in the area of the vortex pair recirculation cell (or jet cross section) occurs due to entrainment of warmer fluid, which necessarily reduces the overall density of the cell.

To represent this density variation, conservation of mass associated with a viscous core of radius a over the time increment dt can be written as

$$\rho_c(t)\pi a^2(t)+\rho_j(t)\pi[a^2(t+dt)-a^2(t)]$$
$$=\rho_c(t+dt)\pi a^2(t+dt)$$

Here the density of the core changes from $\rho_c(t)$ to $\rho_c(t+dt)$, and the core radius changes from $a(t)$ to $a(t+dt)$. By using Eq. (4) for the dependence of a on time, and expanding $\rho_c(t+dt)$ and $a(t+dt)$ in terms of a Taylor series in dt, the following differential equation in the core density is evolved:

$$\frac{d\rho_c}{dt}=\frac{1}{t}(\rho_j(t)-\rho_c(t)) \tag{5}$$

This equation is coupled to the density of the rest of the recirculation cell, ρ_j, which must be described by a similar type of mass balance. As indicated by the dimensions given in Lamb,[11] the time-dependent cross-sectional area of the cell can be expressed in terms of the half-spacing of the vortices, where the area $\cong 4Bh^2(t)$ with $B=2.84$. By performing mass conservation associated with the vortex pair recirculation cell at time $t+dt$, then, we obtain

$$\rho_j(t)[4Bh^2(t)-2\pi a^2(t+dt)]+\rho_\infty[4Bh^2(t+dt)$$
$$-4Bh^2(t)]=\rho_j(t+dt)[4Bh^2(t+dt)-2\pi a^2(t+dt)]$$

representing mixing of the jet fluid at time t with the cross flow (of density ρ_∞) to produce the density $\rho_j(t+dt)$ in the cell. Again, by expanding terms in dt, a differential equation governing $\rho_j(t)$ can be derived:

$$\frac{d\rho_j}{dt}=q(t)(\rho_\infty-\rho_j(t)) \tag{6}$$

where

$$q(t)=\frac{2h(t)(dh/dt)}{h^2(t)-(\pi/2B)a^2(t)}$$

As postulated in the isothermal transverse jet model,[7] vorticity generated at the jet orifice has one component which lies parallel to the jet (arising from flow about the circular orifice) and one which lies parallel to the cross flow (arising from the jet's impulse). Cross-sectional "slices" of the jet taken downstream thus reveal both components, indicating that circulation of each vortex may take the form

$$\Gamma_0(t)=(2U_\infty d)\sin\phi_v(t)+(P/2\rho_\infty h)\cos\phi_v(t) \tag{7}$$

Here, the term $(2U_\infty d)$ approximates the circulation of one of a pair of attached vortices generated by flow about a circular cylinder of diameter d; this term is dominant in the near field.[12] The term $(P/2\rho_\infty h)$ represents the equivalent vortex circulation produced by a jet with impulse per unit depth

$$P=(\rho_{j0}\pi d^2U_j^2)/4U_\infty$$

which by definition lies perpendicular to the jet, thus dominating the far field. Another important assumption made here is that vorticity generation at the orifice is the major contribution to the evolving vortex strength downstream, and that density variation in the jet downstream is a less important influence. Since the problem is largely momentum-dominated, this simplifying assumption should be reasonable.

A nondimensionalization of the parameters in this problem perhaps assists in making clear the nature of the governing equations. Incorporating a characteristic length $L=Rd$ and characteristic time L/U_∞, based on the jet-to-cross flow momentum ratio $R^2=\rho_{j0}U_j^2/\rho_\infty U_\infty^2$, the following dimensionless variables may be defined: $\tilde{h}\equiv h/L$, $\tilde{t}\equiv U_\infty t/L$, $\tilde{\Gamma}_0\equiv\Gamma_0/U_\infty L$, $\tilde{\rho}_j\equiv\rho_j/\rho_{j0}$, $\tilde{\rho}_c\equiv\rho_c/\rho_{j0}$, and $\tilde{\rho}_\infty\equiv\rho_\infty/\rho_{j0}$. The governing equation for dimensionless half-spacing then becomes

$$\frac{d^2\tilde{h}}{d\tilde{t}^2}+\left[\left(\frac{d\tilde{\rho}_c}{d\tilde{t}}+k\frac{d\tilde{\rho}_j}{d\tilde{t}}\right)+\frac{1}{\tilde{t}}(\tilde{\rho}_c+k\tilde{\rho}_j)\right.$$
$$\left.\div(\tilde{\rho}_c+(k-1)\tilde{\rho}_j)\right]\frac{d\tilde{h}}{d\tilde{t}}$$
$$-\left[\frac{\tilde{\rho}_j}{\tilde{\rho}_c+(k-1)\tilde{\rho}_j}\right]\left[\frac{\tilde{\Gamma}_0^2(\tilde{t})}{8\pi^2\tilde{h}^3}\right]\left[1-\frac{C^2\tilde{t}}{(Re)\tilde{h}^2}\right]=0 \tag{8a}$$

with density variation in the cell and cores governed by the relations

$$\frac{d\tilde{\rho}_c}{d\tilde{t}}=\frac{1}{\tilde{t}}(\tilde{\rho}_j-\tilde{\rho}_c) \tag{8b}$$

$$\frac{d\tilde{\rho}_j}{d\tilde{t}}=q(\tilde{t})(\tilde{\rho}_\infty-\tilde{\rho}_j) \tag{8c}$$

where

$$\tilde{\Gamma}_0(\tilde{t})=\frac{\pi^2/2}{\sqrt{(4\pi\tilde{h}-(2/R))^2+(\pi/8\tilde{h})^2}}$$

and

$$q(\tilde{t})=\tilde{h}\frac{d\tilde{h}}{d\tilde{t}}\Big/\left(\tilde{h}^2-\left[\frac{2\pi C^2}{(Re)B}\right]\tilde{t}\right)$$

The nondimensionalization incorporates a Reynolds number based on cross flow velocity and characteristic length, which reduces to

$$Re=U_\infty L/\nu=(U_j d/\nu)(\tilde{\rho}_\infty)^{-1/2}$$

Thus, the differential Eqs. (8a-c) are to be solved simultaneously to yield solutions for vortex pair half-spacing, core density, and cell density as a function of flow time. "Initial" conditions for the problem can be obtained by an asymptotic solution for (8a-c) near $\tilde{t}=0$, yielding

$$\tilde{h}(\tilde{t}_0)=b\tilde{t}_0^{\frac{1}{2}},\quad \tilde{\rho}_c(\tilde{t}_0)=1.0,\quad \tilde{\rho}_j(\tilde{t}_0)=1.0$$

with the coefficient b dependent on the flowfield parameters R, $\tilde{\rho}_\infty$, and Re, as determined by the analysis. The "initial" flow time t_0 corresponds to the actual value of half-spacing h at the jet orifice, found by equating orifice area to recirculation cell area. Based on all of this information, then, solutions for $\tilde{h}(\tilde{t})$, and $\tilde{\rho}_j(\tilde{t})$ can be computed.

Prediction of the dilution jet trajectory can be made from the solution of the dimensionless downstream half-spacing $\tilde{h}(\tilde{t})$ if the local average jet velocity $u_v(t)$ is known. With reference to Fig. 3, a momentum calculation along the jet trajectory can be made, neglecting pressure gradients and gravitational forces. These assumptions have been justified computationally and are appropriate because the problem is momentum-dominated. After a boundary-layer type of evaluation of the equations is made, and nondimensionalization per-

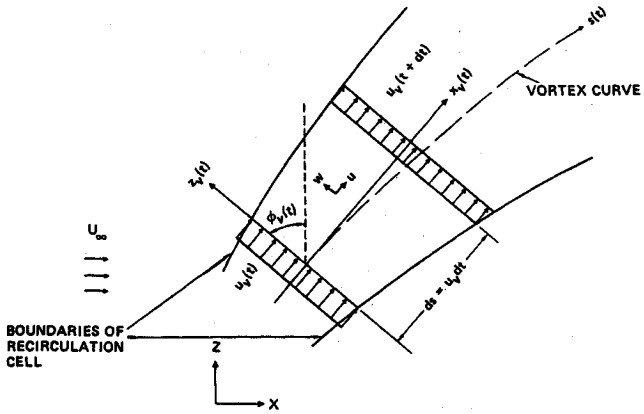

Fig. 3 Flowfield relative to an element *ds* of the vortex pair recirculation cell.

sionalization performed, the following relation governing the jet velocity is derived:

$$\frac{d\tilde{u}_v}{d\tilde{t}} = \left[\frac{\cos\phi_v(\tilde{t}) - R\tilde{u}_v(\tilde{t})}{2R - [\cos\phi_v(\tilde{t})]/\tilde{u}_v(\tilde{t})}\right]\frac{1}{\eta}\frac{d_\eta}{d\tilde{t}} \tag{9}$$

where $\tilde{u}_v \equiv u_v/U_j$, and

$$\eta(t) \equiv \tilde{\rho}_c\left(\frac{8\pi C^2\tilde{t}}{Re}\right) + \tilde{\rho}_j\left(4B\tilde{h}^2 - \frac{8\pi C^2\tilde{t}}{Re}\right)$$

Jet trajectories may now be determined through the geometrical relations for location of the vortex pair in the flowfield:

$$\frac{X(\tilde{t})}{d} = R^2\int_{\tilde{t}_0}^{\tilde{t}} \tilde{u}_v(\tau)\cos\phi_v(\tau)d\tau \tag{10a}$$

$$\frac{Z(\tilde{t})}{d} = R^2\int_{\tilde{t}_0}^{\tilde{t}} \tilde{u}_v(\tau)\sin\phi_v(\tau)d\tau \tag{10b}$$

Results are now obtained numerically using a fourth-order Runge-Kutta scheme; for the single jet with density variation, these results are shown in Figs. 4 through 6. In Figs. 4a-d, the effect of increasing the density of the cold jet over that of the hot cross flow is demonstrated for a given value of momentum ratio R^2. As would be expected, the colder jet penetrates further into the cross flow than an isothermal jet for this momentum-dominated problem. In our model, the reduced lift force F_y due to the presence of warmer fluid in the jet cross section causes the cores to separate more slowly, thus reducing h/d at a given location. Also, because of the decreased rate of core separation here, vortex strength increases in the far field with lower values of $\tilde{\rho}_\infty$, since in the far field the impulse dominates the circulation term. A dimensionless entrainment parameter

$$e \equiv \frac{d}{\rho_{j0}[(\pi/4)d^2U_j]}\frac{d}{ds}[\dot{m}_j(t)]$$

[where $\dot{m}_j(t)$ is the mass flux of fluid in the recirculation cell at time t], representing the degree of entrainment of cross flow, actually decreases as density ratio $\tilde{\rho}_\infty$ is decreased. This occurs again due to the effect of the reduction in the rate of vortex separation.

Based on the governing equations, it is clear that dilution jet trajectories will actually scale with density ratio $\tilde{\rho}_\infty$ as well as the momentum ratio R^2. Least squares curve fitting of our results yields the relation

$$Z/d = \alpha(R)^\beta(\tilde{\rho}_\infty)^\gamma(X/d)^\delta \tag{11}$$

where the parameters α, β, γ, δ are not strictly constants. Average values in the far field ($X/d > 30$) for the ranges

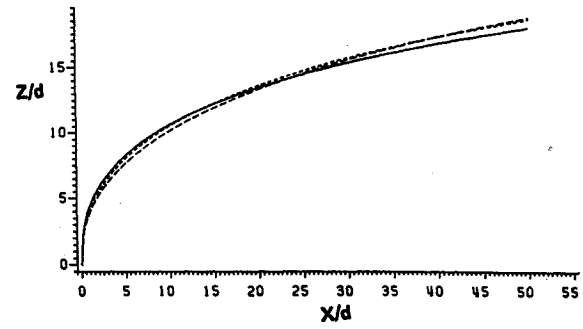

Fig. 4a Effect of density variation for cold jet in hot cross flow: vortex pair trajectories for $R=8$, $\tilde{\rho}_\infty = \rho_\infty/\rho_{j0} = 1.0$ (——), 0.7 (---), and 0.5 (– – –).

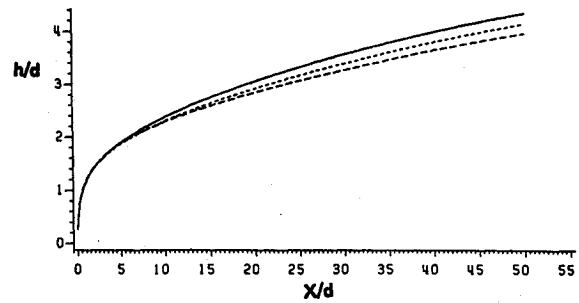

Fig. 4b Effect of density variation for cold jets in hot cross flow: vortex spacing for $R=8$, $\tilde{\rho}_\infty = 1.0$ (——), 0.7 (---), and 0.5 (– – –).

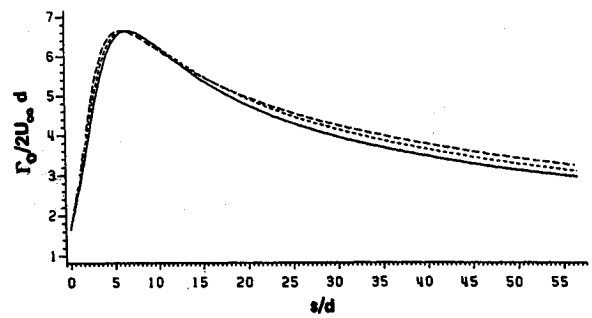

Fig. 4c Effect of density variation for cold jet in hot cross flow: vortex strength for $R=8$, $\tilde{\rho}_\infty = 1.0$ (——), 0.7 (---), and 0.5 (– – –).

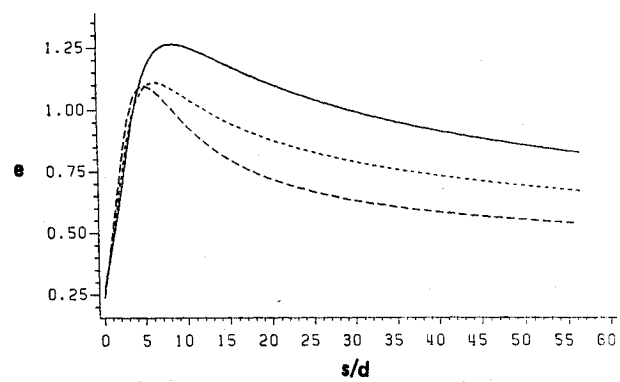

Fig. 4d Effect of density variation for cold jet in hot cross flow: local entrainment for $R=8$, $\tilde{\rho}_\infty = 1.0$ (——), 0.7 (---), and 0.5 (– – –).

$4 < R < 8$ and $0.5 < \tilde{\rho}_\infty < 1.0$ are $\alpha = 0.472$, $\beta = 1.135$, $\gamma = -0.046$, and $\delta = 0.332$. Hence, it appears that the dependence on density ratio is actually secondary.

The hot jet in a cold flow has been studied more frequently in experiments[1,13]; comparison of these results with the present model can also be made. When the density ratio $\tilde{\rho}_\infty$ is greater than unity, the hot jet in a cold cross flow is represented, and there is entrainment of cold fluid by the

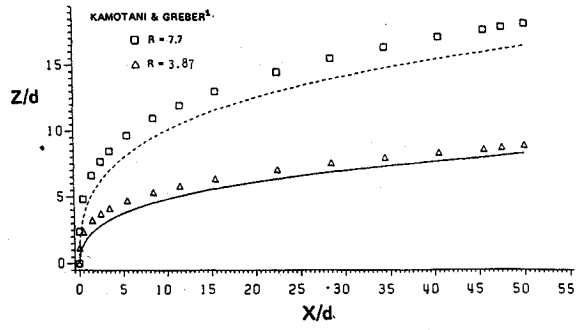

Fig. 5 Vortex pair trajectories for a hot jet in cold cross flow with $\tilde{\rho}_\infty = \rho_\infty/\rho_{j0} = 1.37$, $R = 7.7$ (---), and 3.87 (——) as compared with experimental results (temperature trajectories).

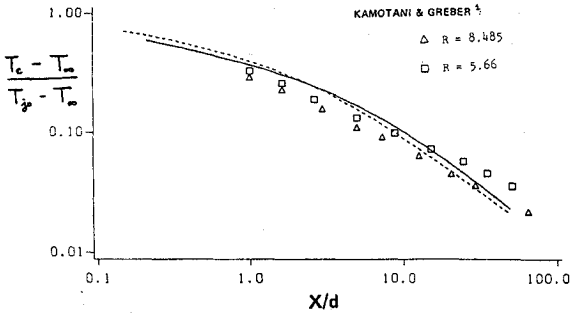

Fig. 6 Dimensionless temperature decay for a hot jet in cold cross flow with $\tilde{\rho}_\infty = \rho_\infty/\rho_{j0} = 1.57$, $R = 8.485$ (——) and $R = 5.66$ (---) as compared with experimental results.

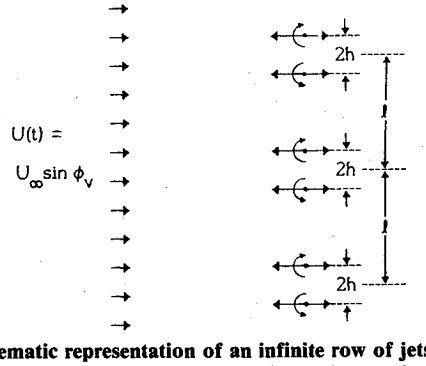

Fig. 7 Schematic representation of an infinite row of jets in a cross flow $U(t)$ with vortex pair half-spacing h and jet spacing ℓ.

warmer cores and jet cross section. Resulting trajectories for this case are shown in Fig. 5, with values chosen for R and $\tilde{\rho}_\infty$ that approximate the experimental values used by Kamotani and Greber.[1] The comparison is made here with experimentally measured maximum temperature trajectories, since these are more closely representative of the location of the vortex cores. The vortex model is fairly successful in its representation, with the scaling law [Eq. (11)] in the range $4 < R < 8$, $1.0 < \tilde{\rho}_\infty < 1.5$ (the heated jet) giving the average quantities $\alpha = 0.48$, $\beta = 1.189$, $\gamma = -0.152$, and $\delta = 0.309$, as compared with values estimated by Kamotani and Greber[1]: $\alpha = 0.73$, $\beta = 1.04$, $\gamma = -0.11$, and $\delta = 0.29$. It should be emphasized that the vortex model here does not employ any empirical constants.

While our model does not explicitly solve for the local jet temperature downstream, a dimensionless temperature decay can be estimated here, assuming temperature to be inversely proportional to local fluid density:

$$\left[\frac{T_c(t) - T_\infty}{T_{j0} - T_\infty}\right] \sim \frac{[(\tilde{\rho}_\infty/\tilde{\rho}_c) - 1]}{(\tilde{\rho}_\infty - 1)}$$

This dimensionless temperature for the viscous core is computed as a function of downstream distance X/d and is shown in Fig. 6. Comparison with measurements by Kamotani and Greber[13] again indicates that approximations made in the present model are appropriate, and that the model represents the dilution jet quite reasonably.

Multiple Jet Model and Results

The situation in which a spanwise row of normally injected dilution jets enter a cross flow of different density introduces additional complications into the behavior of the individual jet. While experiments[13] indicate the presence of vortex pair structures associated with each jet, the dynamics of each vortex will be affected by adjacent vortices. When effectively viewed as a series of successive vortex pairs, the influence of oppositely oriented vortices can be signficant, as shown in Fig. 7. In this diagram, arrows oriented to the left (at each vortex structure) refer to an induced velocity driving the vortex away from the lower wall of the combustor, while an arrow pointing to the right indicates an induction bringing the vortex closer to the lower wall. Hence, the closer the spacing ℓ of the jets in relation to vortex half-spacing h, the greater the influence of adjacent vortices, and the closer the jet trajectories are forced to the injection wall. This trend will continue until the point at which $\ell = 4h$ and the induced velocity of the vortices becomes zero.

Representation of the total induced velocity at a given vortex can be achieved through superposition of the effects of all of the vortices present in the flowfield. If the combustor has a rectangular geometry, with the presence of lateral confining walls, the spanwise row of jets can be considered infinitely long. If the combustor has a circular cross section, an added geometrical factor may be needed; but, for the present we can assume a combustor large enough so that the effects of wall curvature are small. For an infinite row of vortex pairs then, each vortex is affected by an infinite number of vortices, and the total induced velocity at a given vortex may be computed:

$$U_I(t) = (\Gamma_0/4\pi h) + (2\Gamma_0 h/\pi\ell^2) \sum_{m=1}^{\infty} [(2h/\ell)^2 - m^2]^{-1}$$

$$= (\Gamma_0(t)/2\ell)\cot(2\pi h(t)/\ell) \qquad (12)$$

Clearly, in the limit as the jet spacing becomes infinite, the induced upwash velocity is that of the single transverse jet, $\Gamma_0(t)/4\pi h(t)$. As spacing decreases, the induced velocity decreases until $U_I(t) = 0$ when $h(t)/\ell = 1/4$. This represents the situation in which the spacing of the vortices, $2h$, is equal to the distance between adjacent vortices belonging to different pairs, $\ell - 2h$. Since this describes the event where vortex pair recirculation cells actually overlap, blocking cross flow about individual jets, the situation cannot be accommodated by the present model. In fact, Kamotani and Greber[13] note from experiments that when initial spacing-to-diameter ratio is reduced below $\ell/d = 4$, the series of jets actually moves away from the lower wall, similar to a 2D slit behavior. Hence, in our calculations, the condition in which recirculation cells overlap is checked and the specific calculation is terminated, as an indication that the row of jets is approaching the formation of a single, two-dimensional transverse jet.

Computation of forces acting on each vortex core proceeds in the same manner as described for the single dilution jet, yet here an infinite number of vortices and viscous cores must be superposed. It is assumed that relations for vortex strength and core radius are identical to those for the single dilution jet as long as individual jets are distinct. Hence the force F_y acting to separate vortices of a given pair may be

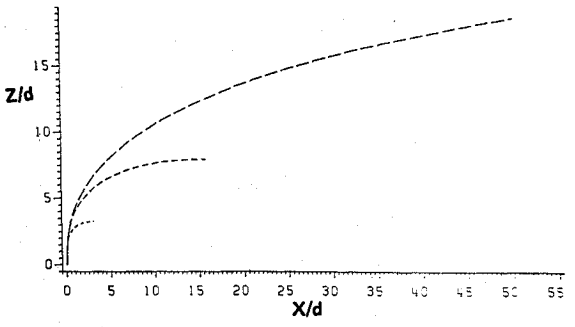

Fig. 8a Multiple dilution jet injection: vortex trajectories for $R=8$, $\tilde{\rho}_\infty=0.7$, $\ell/d=4$ (——), 6 (---), 10 (– – –), and single jet case (———).

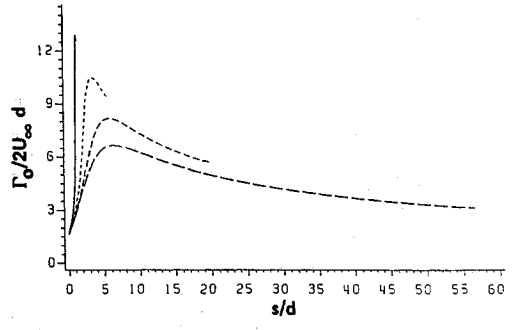

Fig. 8b Multiple dilution jet injection: vortex strength for $R=8$, $\tilde{\rho}_\infty=0.7$, $\ell/d=4$ (——), 6 (---), 10 (– – –), and single jet case (———).

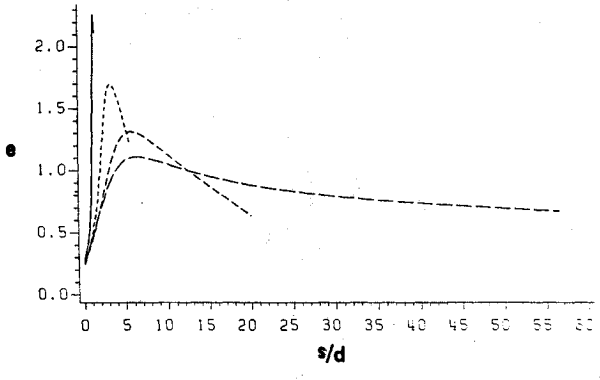

Fig. 8c Multiple dilution jet injection: entrainment coefficient e for $R=8$, $\tilde{\rho}_\infty=0.7$, $\ell/d=4$ (——), 6 (---), 10 (– – –), and single jet case (———).

determined:

$$\frac{F_y}{\text{depth}}=\rho_j\left\{U(t)\Gamma_0-\left(\frac{\Gamma_0^2}{2\ell}\right)\cot\left(\frac{2\pi h}{\ell}\right)\right.$$

$$+\frac{\Gamma_0}{3\ell^2}U(t)\pi a^2+\frac{2\Gamma_0U(t)\pi^2a^2}{\ell^2}\operatorname{cosec}^2\left(\frac{2\pi h}{\ell}\right)$$

$$\left.-4U^2(t)a^4\left(\frac{\pi^4}{\ell^3}\right)\operatorname{cosec}^2\left(\frac{2\pi h}{\ell}\right)\cot\left(\frac{2\pi h}{\ell}\right)+\pi a^2\frac{\mathrm{d}^2h}{\mathrm{d}t^2}\right\}$$

The expression for the component of cross flow velocity $[U(t)=U_\infty\sin\phi_v(t)]$ utilized here must be equal to the upwash velocity of the vortices, $U_I(t)$. With this substitution, an incorporation of a force balance on each vortex core, and appropriate series representations and nondimensionalization (as done previously), a governing equation for dimensionless

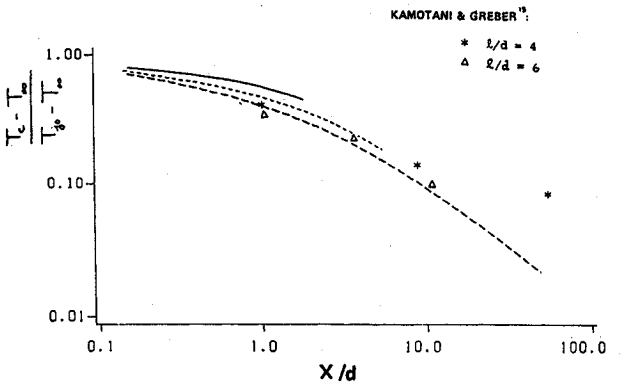

Fig. 9 Multiple heated jet injection: temperature decay for $\tilde{\rho}_\infty=1.57$, $R=5.66$, $\ell/d=4$ (——), 6 (---), single jet (———) as compared with experiments.

half-spacing $\tilde{h}(\tilde{t})$ may be derived:

$$\frac{\mathrm{d}^2\tilde{h}}{\mathrm{d}\tilde{t}^2}+\left[\frac{[(k+1)/(\tilde{t})]\tilde{\rho}_j+kq(\tilde{t})(\tilde{\rho}_\infty-\tilde{\rho}_j)}{\tilde{\rho}_c+(k-1)\tilde{\rho}_j}\right]\frac{\mathrm{d}\tilde{h}}{\mathrm{d}\tilde{t}}$$

$$-\left[\frac{\tilde{\rho}_j}{\tilde{\rho}_c+(k-1)\tilde{\rho}_j}\right]\left[\frac{\tilde{\Gamma}_0^2R^3}{6\tilde{\ell}^3}\right]\cot\left(\frac{2\pi R\tilde{h}}{\tilde{\ell}}\right)$$

$$+\frac{\tilde{\Gamma}_0^2R^3\pi}{\tilde{\ell}^3}\operatorname{cosec}^2\left(\frac{2\pi R\tilde{h}}{\tilde{\ell}}\right)\cot\left(\frac{2\pi R\tilde{h}}{\tilde{\ell}}\right)$$

$$\times\left[1-\frac{4\pi^2C^2\tilde{t}R^2}{\tilde{\ell}^2(Re)}\cot^2\left(\frac{2\pi R\tilde{h}}{\tilde{\ell}}\right)\right]=0 \qquad (13)$$

Again, it should be noted that as the jet spacing ratio $\tilde{\ell}\equiv\ell/d$ becomes infinite, Eq. (13) reduces to the governing equation for the dilution jet [Eq. (8a)] with $a=C\sqrt{4\nu t}$.

Calculation of $h(t)$ now follows from simultaneous numerical solution of Eqs. (13), (8b), and (8c). It is assumed that vorticity generation and entrainment occur by the same mechanisms as for the single transverse dilution jet, but this is clearly less accurate as the jets are more closely spaced. Finally, determination of the local jet velocity $u_v(t)$ is possible by solution of Eq. (9), and correspondence to the trajectory of the row of jets is found using Eqs. (10a) and (10b) for $X(t)$ and $Z(t)$.

Examination of the effects of jet spacing on the cold jet trajectory is shown in Fig. 8. As the spacing ratio is reduced, the trajectory is forced closer to the injection wall, as expected. For these more closely spaced jets, however, the vortices associated with each pair approach adjacent vortices more quickly, and the overall jet trajectory quickly approaches a two-dimensional jet; in fact, this occurs within 5 jet diameters for $\tilde{\ell}=4$ and 6.

In terms of a comparison of our results with experimental data, the hot jet in a cold cross flow again must be considered. Kamotani and Greber[13] are the only researchers, to our knowledge, that have examined multiple jet injection in a cross flow for which the effect of a confining opposite wall may be neglected. Since their jet trajectories are computed from the points of maximum velocity and not from temperature extrema, comparison of the vortex pair trajectory is not possible here; comparison of the downstream temperature decay is possible, however, and this is shown in Fig. 9. While the magnitude of the temperature decay compares favorably in general, these results indicate that the two-dimensional jet behavior is approached fairly quickly for low spacing-to-diameter ratio. As mentioned, computation of the temperatures and trajectories beyond $h/\ell=¼$ is not possible using the vortex model in its present form.

Conclusions

Vortex modeling undertaken here for transverse dilution jet mixing indicates a number of important conclusions that can be drawn. With respect to the single dilution jet, vortex pair trajectories are found analytically to scale with jet-to-cross flow momentum ratio and, to a lesser degree, with jet-to-cross flow density ratio. Scaling is corroborated quite well by experimental findings[13] for a hot jet in cross flow, and downstream temperature decay also is predicted successfully. The cold jet in a hot cross flow has a somewhat different scaling with momentum and density ratios, indicating that, to an extent, the two problems are dissimilar in nature. The hot jet entrains cooler fluid from the cross flow, so that the separation forces are greater on the viscous cores; the exact opposite situation occurs for the cold jet in the hot cross flow, thus reducing the degree of vortex separation.

Multiple (spanwise) jet injection causes the vortices associated with each jet to interact, with the result that the cross flow is penetrated to a far lesser degree overall by the jets. This model indicates that closely spaced jets (e.g., $\ell/d \leq 6$) also approach the behavior of a two-dimensional slit relatively quickly. This model in its present form cannot accomodate this 2D behavior, but does represent the interaction satisfactorily while the jets remain distinct.

Acknowledgments

This work was supported by NASA under Grant NAG 3-543. The authors wish to acknowledge helpful discussions with Dr. James D. Holdeman of NASA Lewis Research Center, Professor Frank E. Marble of the California Institute of Technology, and Dr. William Ashurst of Sandia National Laboratories.

References

[1]Kamotani, Y. and Greber, I., "Experiments on a Turbulent Jet in a Cross Flow," *AIAA Journal*, Vol. 10, Nov. 1972, pp. 1425-1429.

[2]Keffer, J.F. and Baines, W.D., "The Round Turbulent Jet in a Cross-Wind," *Journal of Fluid Mechanics*, Vol. 15, 1963, pp. 481-496.

[3]Holdeman, J.D., Walker, R.E., and Kors, D.L., "Mixing of Multiple Dilution Jets with a Hot Primary Airstream for Gas Turbine Combustors," AIAA Paper 73-1249, Nov. 1973.

[4]Fearn, R. and Weston, R.P., "Vorticity Associated with a Jet in a Cross Flow," *AIAA Journal*, Vol. 12, Dec. 1974, pp. 1666-1671.

[5]Le Grives, E., "Mixing Process Induced by the Vorticity Associated with the Penetration of a Jet into a Cross Flow," *Journal of Engineering for Power*, Vol. 100, July 1978, pp. 465-475.

[6]Holdeman, J.D. and Walker, R.E., "An Empirical Model for the Mixing of a Row of Dilution Jets with a Confined Cross Flow," NASA TM X-71787, 1976.

[7]Karagozian, A.R., "An Analytical Model for the Vorticity Associated with a Transverse Jet," *AIAA Journal*, Vol. 24, March 1986, pp. 429-436.

[8]Karagozian, A.R., "The Flame Structure and Vorticity Generated by a Transverse Fuel Jet," *AIAA Journal*, to be published.

[9]Broadwell, J.E. and Breidenthal, R.E., "Structure and Mixing of a Transverse Jet in Incompressible Flow," *Journal of Fluid Mechanics*, Vol. 148, 1984, pp. 405-412.

[10]Milne-Thomson, L.M., *Theoretical Hydrodynamics*, 5th Ed., MacMillan, New York, 1968, p. 255.

[11]Lamb, H., *Hydrodynamics*, 6th Ed., Dover, New York, 1945, p. 221.

[12]Chang-Lu, H., "Aufrollung unes Zylindrischen Strahles durch Overwind," Ph.D. Dissertation, University of Gottingen, Germany, 1942.

[13]Kamotani, Y. and Greber, I., "Experiments on Confined Turbulent Jets in a Crossflow," NASA CR-2392, March 1974.